

Synthesis, characterization and CO₂ adsorption of Fe(III)-based metal-organic framework

S. U. Rather*, A. Muhammad, A. A. Al-Zahrani, T. E. Youssef, L. A. Petrov

Department of Chemical and Materials Engineering, King Abdulaziz University, P.O. Box 80204, Jeddah 21589, Saudi Arabia

Received, April 17, 2018; Revised, August 7, 2018

Iron (III)-based metal-organic framework (Fe-MOF) was synthesized via solvothermal method utilizing tritopic bridging 1,3,5-Tris(4-carboxyphenyl) benzene as a linker between metal centers. Thermogravimetric analysis revealed that weight loss in the entire temperature range corresponds to loss of desorption of adsorbed gases from pores and cavities, removal of N, N-dimethyl formamide, and framework disintegration. Specific surface area was found to be 300 m²/g and a very little rise in the isotherm at partial pressure > 0.2, indicates microporous character of the sample. Maximum CO₂ adsorption capacity of Fe-MOF sample measured at room temperature and partial pressure of 0.9 atm was found to be 3.0 wt.%. Temperature increase from 298 to 343 K decreases adsorption capacity is related to Le-Chatelier's Principle. Linearity of CO₂ adsorption in a Fe-MOF sample related to weak adsorption sites.

Keywords: Solvothermal, Metal-organic frameworks, Ligand, Surface area, Thermogravimetric analysis, Adsorption

INTRODUCTION

Anthropogenic carbon dioxide discharging from natural and manufactured sources need to mitigate for the sake of pollution free environment. For researchers, scientists and academicians worldwide, an intimidating task lies ahead to reduce greenhouse gases (GHGs) emission from various sources such as combustion of fossil fuels, electricity and heat sector, transportation, industrial processes, deforestation, commercial and residential places [1, 2]. Multiple programs, conferences, and seminars are held worldwide to make people aware about harmful effects of GHGs emission especially CO₂, a primary source of global warming. Combustion of fossil fuels and industrial processes are responsible for 65% of CO₂ emission worldwide. Moreover, combustion of fossil fuels such as coal, natural gas, and oil in USA alone produces 83% of GHGs emissions. Recently different type of methods are utilized to separate CO₂ from fossil fuel gas emissions and one of the main method to reduce CO₂ emission is adsorption [3, 4]. Physical and chemical adsorption methods are widely used to separate CO₂ from mixture [5, 6].

High selectivity, high porosity, tunable property, low cost, good mechanical strength, stable adsorption capacity post many cycles, and sufficient adsorption/desorption kinetic properties are mandatory parameters to adsorb CO₂ efficiently. Functionalized carbon materials, carbon-based nanomaterials, pyrogenic carbons, and carbon composites used as adsorbents for CO₂ capture at low temperature and moderate pressure

[4, 7-10]. Zeolites also used for CO₂ adsorption owing to its unique high porous characteristics, open cavities in the form of channels and cages, and well-defined structures [11, 12]. Porous metal-organic frameworks (MOFs) also known as coordination polymer considered as promising adsorbent for CO₂ adsorption [13]. MOFs are blend of organic and inorganic mixture of metal ions or clusters coordinated to one or more than one type of ligands to form network type structures [14, 15]. MOFs display wide diversity and structural disparity in combination with lower topological restrictions on the formation of three-dimensional frameworks [16]. High surface area, permanent porosity, stability, and functionalization are unique characteristics of MOFs [17].

Excessive surface area and variable pore structure MOFs synthesized by solvothermal and non-solvothermal, microwave, electrochemical, mechanochemical, and sonochemical methods [14, 18-20]. For the preparation of 3D network type MOF structures, different kinds of metal or metal oxide (polyhedral) clusters with unique neutral, cationic, and anionic organic ligands with rigid backbones such as pyrazine, bipyridine, carboxylates, and imidazole are used [19]. Generally, for the preparation of various kinds of MOFs, heating a mixture of metal salt and organic ligands in a solvent such as water, ethanol, diethylformamide, and dimethylformamide routes are used [14, 20, 21]. Preparation of MOF-177 via solvothermal method by employing zinc acetate/zinc nitrate as a metal center and tritopic

* To whom all correspondence should be sent:

E-mail: rathersami@kau.edu.sa;

rathersami@gmail.com

organic ligand benzene tribenzoic acid (BTB) as a linker in the presence of solvent DEF/DMF are used [22, 23]. Furthermore, synthesis of MOF-39 by connecting zinc oxide metal centers by trigonal organic linker BTB are also prepared by solvothermal method [24].

In this report, convenient solvothermal method are utilized for the preparation of Fe(III)-based metal-organic framework (Fe-MOF) using a reaction involving iron nitrate nonahydrate metal salt as precursor and tritopic 1,3,5-Tris(4-carboxyphenyl) benzene as a linker. Thermal stability and surface area of Fe-MOF measured by thermogravimetric and nitrogen adsorption/desorption isotherms. The CO₂ adsorption capacity of Fe-MOF calculated at 25, 30, 40, 50, 60, 70°C and low pressure 0.0 to 0.9 bar using thermogravimetric analysis method.

EXPERIMENTAL

Synthesis of Iron-based Metal-Organic Framework (Fe-MOF)

Iron nitrate nonahydrate (99%), 1, 3, 5-tris (4-carboxyphenyl) benzene (>98%), ethanol (99.8%), N, N-dimethylformamide (99.8%), and chloroform (>99.5%) were purchased from Sigma-Aldrich and were used without further purification. The synthesis of Fe-MOF performed via solvothermal method. In a typical procedure, 0.270 g iron nitrate nonahydrate was dissolved in 25 ml ethanol, whereas 0.2 g 1,3,5-tris(4-carboxyphenyl) benzene was dissolved in 10 ml N, N-dimethylformamide (DMF). Mixture of above solutions transferred to teflon-lined autoclave and heated at 80°C for 3 days. The reaction mixture cooled slowly to RT and hereafter called as Fe-MOF. The resulting precipitate filtered, washed with DMF to separate some traces of unreacted reagent. Finally, DMF reacted sample washed many times with chloroform to reduce presence of DMF inside crystals. The sample was dried and stored within glove box under Ar atmosphere. Further experimental details of synthesis method presented elsewhere [25]. Fe-MOF was characterized using Fourier-transform infra-red (FT-IR) and scanning electron microscopy (SEM). Nitrogen adsorption performed at 77 K using Micromeritics ASAP 2000 instrument.

CO₂ adsorption capacity measurements of Fe-MOF sample performed by thermogravimetric analysis (TGA) (NETZSCH-Gerätebau GmbH, TG 209 F3) instrument. ~30 mg of Fe-MOF sample used in each CO₂ adsorption experiment. Prior to each adsorption, a sample was stationed in an alumina crucible fixed in TGA furnace and heated

to 100°C (10°C/min.) in a flowing nitrogen (100 ml/min.) and retain at that temperature until a constant weight of sample was obtained. This process for continuing flowing nitrogen at 100°C for 1 h is to ensure the surface of Fe-MOF sample is clean prior commencing adsorption experiments. At constant RT, a gas mixture of 90% CO₂-10% He (100 ml/min.) was released into sample holder holding sample. The increase in weight perceived due to adsorption of CO₂ and preserved until equilibrium was established. Under these conditions, adsorption uptake of CO₂ was determined as the amount of CO₂ adsorbed in milligrams per gram of Fe-MOF (mg CO₂/g Fe-MOF). Adsorption data for other experiments obtained in a similar manner using helium as an inert carrier.

RESULTS AND DISCUSSION

Schematic illustration synthesis of Fe-MOF used to understand the structure of Fe-MOF presented in Fig.1. Iron nitrate an inorganic compound comprising of iron, nitrate and varying number of water molecules attached is used as a metal center (Fig. 1(a)) and 1,3,5-Tris(4-carboxyphenyl) benzene (H₃BTB), a tritopic bridging ligand acts as a linker between metal center (Fig. 1 (b)). One of the Fe³⁺ is coordinated to nine oxygen atoms, where seven of the coordinated oxygen atoms belongs to different BTB³⁻ ligands and two oxygen atoms belongs to terminal water molecules (Fig. 1(d)). Cross-sectional view of Fe-MOF generated from Fig.1 (c) and (d) displaying 1D porous channels between metal central layers (Fig. 1(e)).

Thermal behavior of Fe-MOF calculated using thermogravimetric and differential thermal analysis (DTA). Fixed mass of sample independently heated in an inert atmosphere using a heating ramp of 10°C/min in the temperature range of 25 to 800°C. Fig. 2 (a) and (b) represents thermogravimetric and differential analysis profile of Fe-MOF. Visible continuous decrease in weight loss in the entire temperature range observed [26-29]. ~45.0 wt.% weight loss was observed in the temperature range of 50–250°C and can be attributed to desorption of adsorbed gases from their pores and cavities and loosely bound water molecules [30, 31]. Sample weight loss ~22.0 wt.% observed in the temperature range of 250-500°C corresponds to removal of guest molecules such as N, N dimethyl formamide and adsorbed water molecules from atmosphere. Moreover, above weight loss also indicates initiation of decomposition of Fe-MOF sample [25]. Pore and cavity texture further improved possibly by degassing at elevated temperature for a longer period. Weight loss ~15 wt.% above 500°C

indicates complete disintegration of framework including ligand BTB. The T_{max}, i.e. the temperature at which rate of losing water or adsorbed water molecules or guest molecules or disintegration of MOF is maximum and is calculated from differential thermal analysis. The

T_{max} for losing water, adsorbed water/guest molecules, and disintegration of MOF was 117, 470 and 704°C presented in Fig. 2 (b). Total weight loss observed in the entire temperature range is ~82 wt.% and remaining residue corresponds to oxides of metal center.

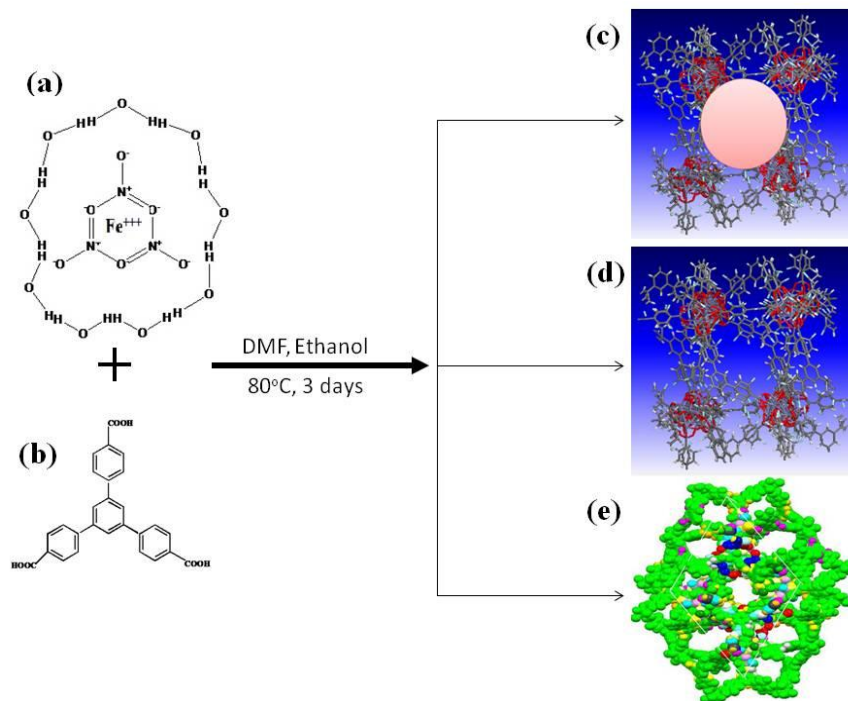


Fig. 1. Schematic illustration preparation method of Fe-MOF, where (a) iron nitrate nonahydrate metal salt as a precursor, (b) tritopic 4,4',4''-benzene-1,3,5-triyl-tribenzoic acid (H₃BTB) ligand as a linker, and (c) , (d) and (e) are three different structural forms of Fe-MOF.

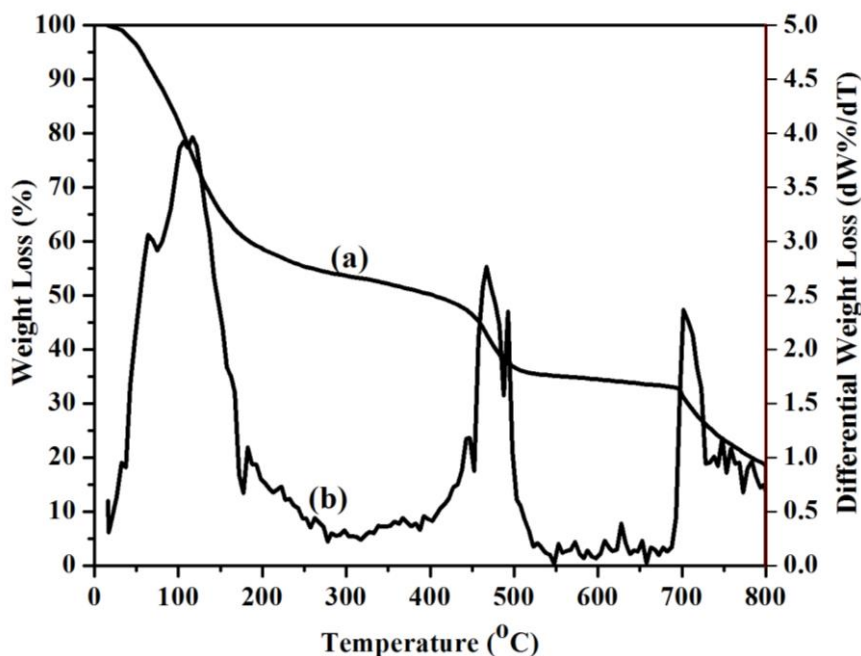


Fig. 2. Thermogravimetric and differential profiles of Fe-MOF, performed in an oxygen atmosphere using ramp rate 10°C/min.

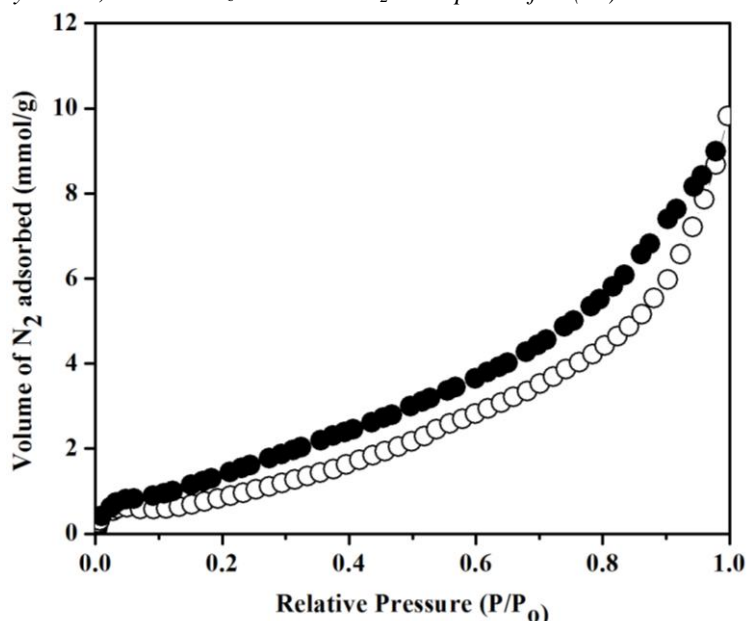


Fig. 3. Nitrogen adsorption/desorption isotherm of Fe-MOF recorded at 77K.

Brunauer–Emmett–Teller (BET) surface area and pore size distribution of sample measured from nitrogen adsorption/desorption profile using Micromeritics ASAP 2000 instrument. The nitrogen adsorption isotherm of Fe-MOF sample carried out by keeping the sample isothermal at 77 K. Fig. 3 presented nitrogen adsorption isotherm of sample. According to the IUPAC classification, the evolution of adsorption isotherm with increasing P/P_0 described as a type II isotherm indicating microporous structure of sample. There is a very little rise in the isotherm at partial pressure > 0.2 , indicating very high microporous density. For relative pressure between 0.1 and 1.0, a gradual rise in the volume of the nitrogen adsorption observed. The specific surface area estimated from linear fit to the BET adsorption isotherm, for the relative pressure range P/P_0 0.0 to 1.0 found to be 300 m²/g.

FT-IR spectra of Fe-MOF synthesized by solvothermal method presented in Fig. 4. Several intense bands throughout the spectrum in agreement with the literature observed. Strong band that appears at 1400 cm⁻¹ is assigned to symmetric (ν_s) stretching of C=O bond related to carboxylate group of ligand BTB and asymmetric (ν_{as}) stretching of same also existed at ~1600 cm⁻¹ region. The C=C bond attributed to stretching vibrations of BTB linker appears at ~1500 cm⁻¹ region. Small peaks visible at 1300-100 cm⁻¹ region corresponds to in-plane bending vibrations of

aromatic C-H bonds while as weak peaks appeared at 1000-800 cm⁻¹ attributed to out of plane bending vibrations of C-H bonds. First overtone of in- and out of plane vibrations of C-H bonds of ligand BTB appears at ~1600-2000 cm⁻¹, whereas in- and out of plane vibrations of C-H bonds appears at ~2600-2100 cm⁻¹[32-34]. SEM images presented in Fig. 5 (a) and (b) indicates morphological characterization of Fe-MOF sample. Crystal structure images presented resembles trigonal lattices with average diameter of 6.76 μm .

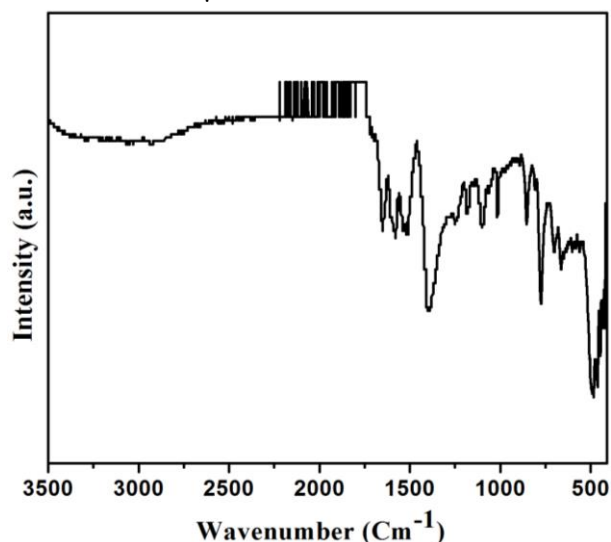


Fig. 4. Fourier-transform infrared (FTIR) spectra of Fe-MOF sample.

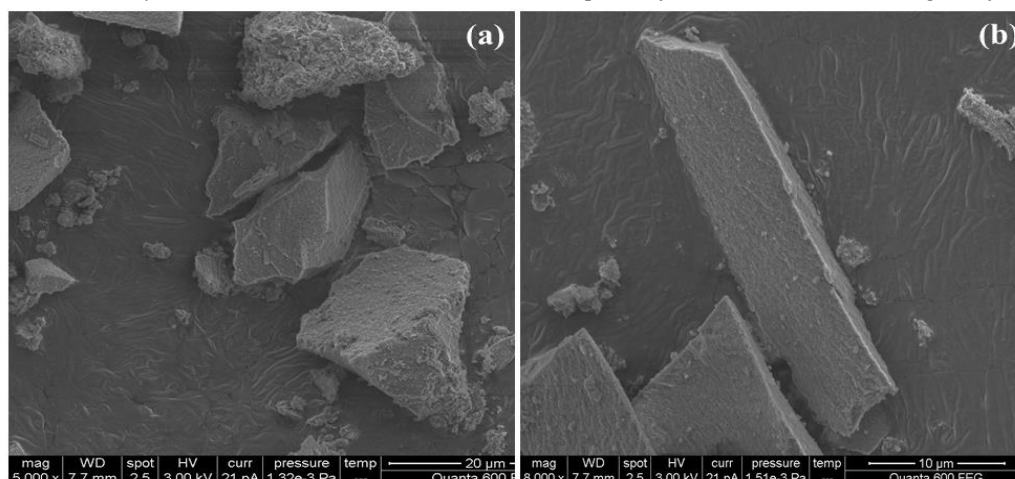


Fig. 5. Representative scanning electron microscope (SEM) images of Fe-MOF. The scale bar for (a) and (b) is 20 and 10 μm, respectively.

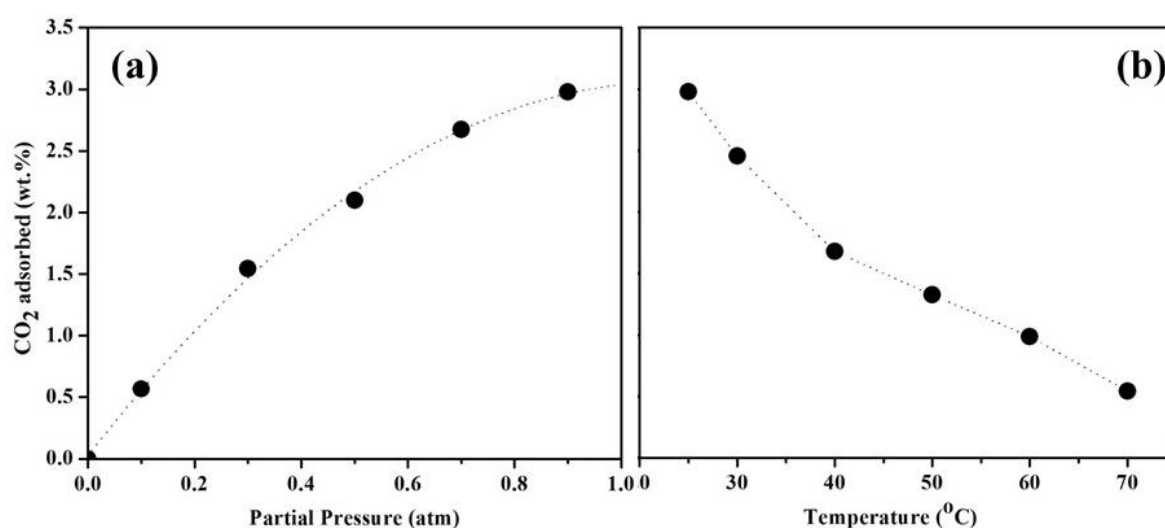


Fig. 6. (a) CO₂ adsorption capacity of Fe-MOF sample performed at 25°C and partial pressure range of 0.0 and 0.9 atm. (b) CO₂ adsorption of Fe-MOF sample performed at 25, 30, 40, 50, 60, and 70°C and pressure 0.9 atm.

Considering highly porous nature of Fe-MOF sample, CO₂ adsorption capacity measurements presented in Fig. 6 (a) and (b) performed at different temperatures and partial pressure range of 0.0 and 0.9 atm. Sample follows monotonous type CO₂ adsorption isotherm (type I) and adsorption is limited to few molecular layers only. At low pressure, gradual rise of CO₂ adsorption observed and at high pressure, linear adsorption indicating adsorption sites on Fe-MOF are weak and relatively homogeneous. Maximum CO₂ adsorption capacity of sample found to be ~3.0 wt.% at 298 K and partial pressure of 0.9 atm. The CO₂ adsorption capacity of our sample very low compared to adsorption literature data of various types of MOFs and reason may be poor BET surface area. Moreover, as far as high gas adsorption capacity is concerned, high surface area is mandatory. Temperature elevation from 25 to

70°C decreases CO₂ adsorption capacity of Fe-MOF (Fig. 6(b)). Furthermore, reduction of adsorption capacity with decreasing temperature is due to Le Chatelier's principle. The CO₂ adsorption capacity data obtained fitted to Langmuir adsorption isotherm to estimate maximum adsorption (q_m) and adsorption equilibrium constant (K) according to the Langmuir adsorption equation:

$$q_e = q_m \frac{Kp_e}{1 + Kp_e}$$

where p_e is the equilibrium partial pressure of CO₂. Polymath, a nonlinear regression software used to determine Langmuir equation parameters q_m , K, and correlation coefficient (R^2) as a statistical indicator of goodness of model prediction.

CONCLUSION

Fe-MOF synthesized by solvothermal method using tritopic ligand H₃BTB as a linker to study structural, thermal, morphological, and CO₂ adsorption properties. Thermal profile of Fe-MOF shows continuous weight loss in the entire temperature range of RT to 800°C. Furthermore, weight reduction of sample corresponds to loss of loosely bound water molecules attached to metal center and ligands, within cavities and channels, adsorbed water molecules, guest molecules such as DMF and MOF disintegration. Specific surface area of Fe-MOF found to be 300 m²/g and little rise in the isotherm at partial pressure > 0.2, indicating very high microporous density. The CO₂ adsorption capacity of Fe-MOF was found to be 3.0 wt.% at 298 K and partial pressure of 0.9 atm. Furthermore, CO₂ adsorption decreases as the temperature increases follows Le-Chatelier's Principle. The CO₂ adsorption capacity increases linearly with pressure indicating adsorption sites on sample are weak and relatively homogeneous.

Acknowledgements: This project was funded by the Deanship of Scientific Research (DSR), King Abdulaziz University, Jeddah, under grant No. (1434/135/494). The authors, therefore, acknowledge with thanks DSR technical and financial support.

REFERENCES

- J. H. Edwards, *Catal. Today* **23**, 59 (1995).
- M. R. Raupach, G. Marland, P. Ciais, C. Le Quere, J. G. Canadell, G. Klepper, C. B. Field, *Proc. Natl. Acad. Sci. U.S.A* **104**, 10288 (2007).
- Z. Liang, M. Marshall, A. L. Chaffee, *Energ. Fuel* **23**, 2785 (2009).
- D. Cazorla-Amoro's, J. Alcaniz-Monge, A. Linares-Solano, *Langmuir* **12**, 2820 (1996).
- M. Ishibashi, H. Ota, N. Akutsu, S. Umeda, M. Tajika, J. Izumi, A. Yasutake, T. Kabata, Y. Kageyama, *Energy Convers. Mgrat.* **37**, 929 (1996).
- Y. Liu, Y. Yang, Q. Sun, Z. Wang, B. Huang, Y. Dai, X. Qin, X. Zhang, *ACS Appl. Mater. Interfaces* **5**, 7654 (2013).
- Z. Yong, V. Mata, A. E. Rodrigues, *Sep. Purif. Technol.* **26**, 195 (2002).
- N. P. Wickramaratne, M. Jaroniec, *ACS Appl. Mater. Interfaces*, **5** 1849 (2013).
- R. V. Siriwardane, M. S. Shen, E. P. Fisher, J. A. Poston, *Energ. Fuel* **15**, 279 (2001).
- F. Su, C. Lu, W. Cnen, H. Bai, J. F. Hwang, *Sci. Total Environ.* **407**, 3017 (2009).
- P. D. Jadhav, R. V. Chatti, R. B. Biniwale, N. K. Labhsetwar, S. Devotta, S. S. Rayalu, *Energ. Fuel* **21**, 3555 (2007).
- D. Bonenfant, M. Kharoune, P. Niquette, M. Mimeault, R. Hausler, *Sci. Technol. Adv. Mater.* **9**, 013007 (2008).
- P. L. Llewellyn, S. Bourrelly, C. Serre, A. Vimont, M. Daturi, L. Hamon, G. D. Weireld, J. S. Chang, D. Y. Hong, Y. K. Hwang, S. H. Jung, G. Ferey, *Langmuir* **24**, 7245 (2008).
- N. Stock, S. Biswas, *Chem. Rev.* **112**, 933 (2012).
- S. L. James, *Chem. Soc. Rev.* **32**, 276 (2003).
- J. L. C. Rowsell, O. M. Yaghi, *Micropor. Mesopor. Mat.* **73**, 3 (2004).
- H. Furukawa, N. Ko, Y. B. Go, N. Aratani, S. B. Choi, E. Choi, A. Ö. Yazaydin, R. Q. Snurr, M. O'Keeffe, J. Kim, O. M. Yaghi, *Science* **329**, 424 (2010).
- Y. Sun, H. Zhou, *Sci. Technol. Adv. Mater.* **16**, 054202 (2015).
- Y. R. Lee, J. Kim, W. S. Ahn, *Korean J. Chem. Eng.* **30**, 1667 (2013).
- O. Shekhah, H. Wang, S. Kowarik, F. Schreiber, M. Paulus, M. Tolan, C. Sternemann, F. Evers, D. Zacher, R. A. Fischer, C. Woll, *J. Am. Chem. Soc.* **129**, 15118 (2007).
- A. D. Burrows, K. Cassar, R. M. W. Friend, M. F. Mahon, S. P. Rigby, J. E. Warren, *Cryst. Eng. Comm.* **7**, 548 (2005).
- S. Proch, J. Herrmannsdörfer, R. Kempe, C. Kern, A. Jess, L. Seyfarth, J. Senker, *Chem. Eur. J.* **14**, 8204 (2008).
- D. J. Tranchemontagne, J. R. Hunt, O. M. Yaghi, *Tetrahedron* **64**, 8553 (2008).
- J. Kim, B. Chen, T. M. Reineke, H. Li, M. Eddaoudi, D. B. Moler, M. O'Keeffe, O. M. Yaghi, *J. Am. Chem. Soc.* **123**, 8239 (2001).
- D. Saha, R. Zacharia, L. Lafi, D. Cossement, R. Chahine, *Chem. Eng. J.* **171**, 517 (2011).
- A. R. Chowdhuri, D. Bhattachary, S. K. Sahu, *Dalton Trans.* **45**, 2963 (2016).
- T. H. Chen, A. Schneemann, R. A. Fischer, S. M. Cohen, *Dalton Trans.* **45**, 3063 (2016).
- P. V. Dau, L. R. Polanco, S. M. Cohen, *Dalton Trans.* **42**, 4013 (2013).
- B. X. Dong, L. Chen, S. Y. Zhang, J. Ge, L. Song, H. Tian, Y. L. Teng, W. L. Liu, *Dalton Trans.* **44**, 1435 (2015).
- J. Tang, M. Yang, W. Dong, M. Yang, H. Zhang, S. Fan, J. Wang, L. Tana, G. Wang, *RSC Adv.* **6**, 40106 (2016).
- A. Tăbăcaru, S. Galli, C. Pettinari, N. Masciocchi, T. M. McDonald, J.R. Long, *Cryst. Eng. Comm.* **17**, 4992 (2015).
- T. V. N. Thi, C. L. Luu, T. C. Hoang, T. Nguyen, T. H. Bui, P. H. D. Nguyen, T. P. P. Thi, *Adv. Nat. Sci.: Nanosci. Nanotechnol.* **4**, 035016 (2013).
- D. Ge, J. Peng, G. Qu, H. Geng, Y. Deng, J. Wu, X. Cao, J. Zheng, H. Gu, *New J. Chem.* **40**, 9238 (2016).
- S. He, Z. Li, J. Wang, P. Wen, J. Gao, L. Ma, Z. Yang, S. Yang, *RSC Adv.* **6**, 49478 (2016).

СИНТЕЗ, ОХАРАКТЕРИЗИРАНЕ И СО₂ АДСОРБЦИЯ ВЪРХУ МЕТАЛ-ОРГАНИЧНА МРЕЖА НА ОСНОВАТА НА Fe(III)

С. У. Ратер*, А. Мухамад, А. А. Ал-Захрани, Т. Е. Юсеф, Л. А. Петров

Департамент по инженерна химия и химия на материалите, Университет „Крал Абдулазиз”, п.к. 80204, Джеда 21589, Саудитска Арабия

Постъпила на 17 април, 2018; коригирана на 7 август, 2018

(Резюме)

Метал-органична мрежа (MOF) на основата на Fe (III) е получена по солвотермичен метод с помощта на триопичен мостов лиганд 1,3,5-трис (4-карбоксифенил) бензен като свързващо звено и хром като метал, образуващ вторична градивна част. Непрекъснатата загуба на тегло в цялата температурна област е свързана с загуба чрез десорбция на адсорбирани газове от порите и кухините, отстраняване на молекули-гости като N, N-диметилформамид (DMF) и дезинтеграция на мрежата. Специфичната площ от 420 m²/g и рязкото нарастване на изотермата при парциално налягане >0.2 atm свидетелстват за микропорестия характер на пробата. Адсорбционният капацитет на Fe-MOF, измерен при 298 K и парциално налягане 0.9 atm, е 3.5 wt.%. Повишаването на температурата от 298 до 343 K понижава адсорбционния капацитет съгласно принципа на Le Chatelier. Адсорбцията на CO₂ нараства линейно с повишаване на налягането от 0 до 0.9 atm поради сравнително слабите адсорбционни центрове и тяхната хомогенност.